Avni Fakioglu, Dursun Özyürek* and Ramazan Yilmaz

Effects of Different Heat Treatment Conditions on Fatigue Behavior of AA7075 Alloy

Abstract: In this study, the effect of different heat treatment processes applied to AA7075 alloys on the fatigue behavior was examined. The processes applied to AA7075 aluminum included annealing (O), high temperature pre-precipitating (HTPP), artificial aging (T6), retrogression and re-aging (RRA). The annealing heat treatment was performed for 2 hours at 500°C and samples were cooled in the furnace. In the artificial aging (T6) process, after the samples were solution treated for 2 hours at 500°C, they were quenched at room temperature and aged for 24 hours at 120°C. In the retrogression and re-aging process, samples were solution treated for 1 hour at 220°C after the T6 process and then re-aged for 24 hours at 120°C. In the high temperature pre-precipitating, pre-precipitates were formed for 30 minutes at 450°C and then, it was aged for 24 hours at 120°C. All samples were characterized through the scanning electron microscope (SEM + EDS), hardness measurements and X-ray difraction (XRD) techniques. At the end of experimental studies, SEM and EDS examinations XRD results revealed that η ($MgZn_2$) phase formed in the microstructure following the HTTP, RRA and T6 heat treatment processes. As a result of the fatigue tests, the highest fatigue strength was measured in samples treated with artificial aging (T6), the lowest fatigue strength was measured in the annealed (O) samples.

Keywords: AA7075 alloy, different heat treatments, fatigue behavior

***Corresponding author: Dursun Özyürek:** Karabuk University, Technology Faculty, Manufacturing Engineering, Karabuk 78100, Turkey. E-mail: dozyurek@karabuk.edu.tr
Avni Fakioglu: Karabuk University, Technology Faculty, Manufacturing Engineering, Karabuk 78100, Turkey
Ramazan Yilmaz: Sakarya University, Technology Faculty, Materials and Metallurgy Engineering, Sakarya 54187, Turkey

1 Introduction

High-strength 7xxx series aluminum alloys are commonly used in the sector of aerospace owing to their features of low density, perfect strength etc. In recent years, studies carried out to improve some characteristics (for instance corrosion) of these alloys including strength by using different processes have increased considerably [1–3]. The most common method used to improve strength in Al-Zn-Mg-Cu alloys is aging treatment. Strength values of 7xxx series alloys can be increased significantly with various heat treatment processes [4–9]. While 7xxx series alloys gain high strength under the artificial aging (T6) conditions, they become considerably sensitive towards stress corrosion. Thus, in order to equilibrate both mechanical properties and corrosion sensitiveness under optimal conditions, 7xxx series alloys are treated with retrogression and re-aging (RRA) and high temperature pre-precipitate (HTPP) aging processes following the T6 heat treatment [5, 10–12].

In T6 heat treatment, precipitates formed in the structure through aging following the dissolution and quenching processes increase the strength of the alloy. The precipitate resulting from the aging of saturated solid solution is formed with the following reaction [13–15].

Saturated solid solution → GP zones → ή ($MgZn_2$) → η ($MgZn_2$). GP zones which have low interfacial energies and in turn, can be produced at low temperatures, are coherent with the matrix and spheric. In the progressive stages of aging, firstly they grow and semi-coherent, instable and monoclinic ή ($MgZn_2$) phase is formed while incoherent, stable and hexagonal η ($MgZn_2$) phase is formed in the last stage [9]. Besides, with the heat treatment, orthorombic S (Al_2CuMg) phase and T ($Al_{32}(Mg,Zn)_{49}$ cubic phase nucleate in the structure at the stage of cooling following the solution process [16]. In many studies, the effect of precipitates formed through aging on the mechanical properties of 7000 series alloys was investigated [17–19].

It is of vital importance to determine the reaction of the material to repeated loads in order to understand the fatigue behavior and microstructural changes displayed

by AA7075 alloy towards variable loadings. In the aged AA7075 alloy, fatigue cracks start from precipitates formed in the structure through aging rather than slipping bands [20]. Fatigue cracks in the matrix start with the breaking of second phase particulates following the repeated loadings and these fatigue cracks formed with the effect of loadings continue growing along the particulate boundries or within the particulates. Precipitates rich in Mg formed in the structure through aging under a uniform and homogeneous deformation act as barrier against dislocation and cross slip movement [21].

In this study, fatigue behaviors of the AA7075 alloy aged through three different heat treatment processes were tested and the obtained results were compared. The present study aimed at determining the fatigue behaviour and its fracture characteristics of the alloy aged through different methods as well as the effect of precipitates formed in the matrix through aging depending on the heat treatment process on the damage tolerance.

2 Materials and methods

In the experimental studies, the AA7075 aluminum alloy that is commonly used in the sector of space and aerospace owing to its specific weight, high strength, electrical and thermal conductivities was used in the experimental studies. Chemical composition of the AA7075 alloy used in the experimental studies is given in the Table 1. The alloy to be used in the experiments was annealed for 2 hours at 500°C (at a heating rate of 10°C/min) prior to the aging processes.

Zn	Mg	Cu	Fe	Cr	Si	Mn	Ti	Al
5,16	2,19	1,30	0,28	0,19	0.17	0.15	0,009	Balance

Table 1: Chemical composition of the AA7075 aluminum alloy

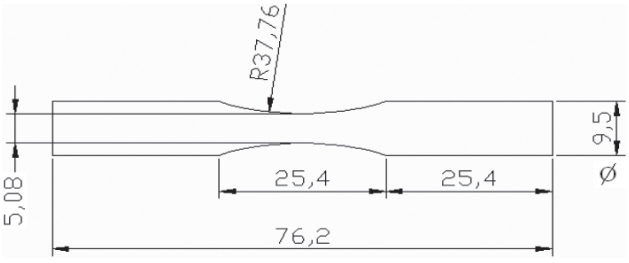

Fig. 1: Dimensions of fatigue test samples used in the experiments

An annealed stick AA7075 aluminum alloy of 10 mm in diameter was treated sensitively in the turning machine and fatigue samples were prepared according to the measurements given in Figure 1 in line with ASTM E-606 standards.

Heat treatment parameters used in the experimental studies were given in Table 2. As it is understood from Table 2, three different heat treatment processes were applied to the prepared fatigue samples.

Annealing (O) was applied to the first group of samples, T6 was applied to the second group of samples, RRA was applied to the third group of samples and HTPP heat treatment was applied to the fourth group of samples. In T6 heat treatment, samples were water quenched after they were solution treated for 2 hours at 485°C and then a 24-hour aging process was performed at 120°C. In RRA process, samples were firstly treated with T6 process, solution treated once more at 220°C 1 hour and then quenched at room temperature in salt water. Afterwards, re-aging was performed for 24 hours at 120°C. As to the HTPP heat treatment, after samples were solution treated, a pre-precipitate formation process was carried out for 30 minutes at 450°C and samples were aged for 24 hours at 120°C. The heating rate of 10°C/min. was used in the

Heat Treatment	Solution temperature and time	Cooling	Pre-precipitating process	Aging	Retrogression (R)	Quenching	Reaging (RA)
T6	485°C 2 hours	Water 25°C	Water 25°C	120°C 24 hours			
T6+RRA	485°C 2 hours			120°C 24 hours	220°C 1 hour	25°C Salt water	120°C 24 hours
HTPP	485°C 2 hours	Furnace	450°C 30 minutes	120°C 24 hours			
O	500°C 2 hours	Furnace					

Table 2: Heat treatment parameters applied to the AA7075 aluminum alloy

aging heat treatments. Standard metallographic processes were applied to all samples for microstructure examinations. In the characterisation studies, scanning electron microscope (SEM) and energy dispersive spectroscopy (EDS) were used while Bruker brand X-Ray diffractometer (XRD) was used in the identification of phases formed in Al matrix at the end of heat treatment. Hardness values of aged samples were measured as Brinell (HB). 5 measurements were made for each sample and the average of these five values was calculated. A ball diameter of 2.5 and charge ratio of 31.25 (2.5/31.25) was used in the hardness measurements.

With the aim of improving the surface quality of samples prepared for fatigue tests, their surfaces were lustered with 3 μm diamond solution following the heat treatment application. A special attention was paid to keep this quality equal in all samples. Rotary tilt test device developed by taking Wöhler type fatigue test device as model was used in the tests. With this device, all tests were carried out at room temperature as 46 frequency (2780 cycles/min.) and R (strain rate) = 1. Five different strain values (200–250–300–350–400 MPa) were used in the fatigue tests. Five different fatigue samples were tested for each load. Fatigue tests were maintained until the samples are broken. At the end of fatigue tests, fractured surfaces of samples were examined through SEM. Wöhler type fatigue test device used in the experiments is demonstrated schematically in Figure 2.

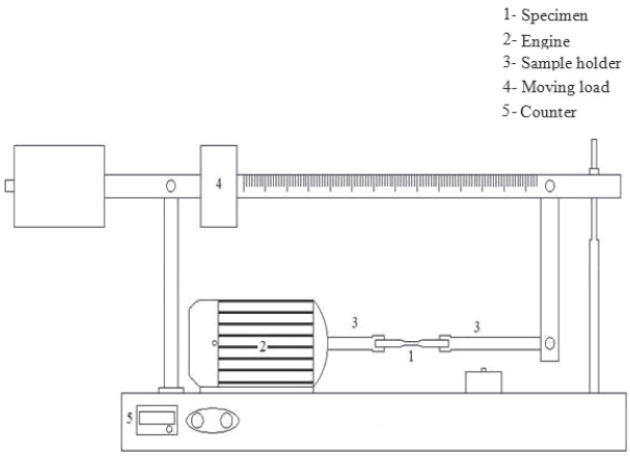

Fig. 2: Schematic image of the rotary tilt fatigue test device

3 Results and discussion

3.1 Microstructure examinations

SEM images of annealed (O), aged (T6), solution re-treated and re-aged (RRA) and pre-precipitated (HTPP) samples of the AA7075 alloy treated with different heat treatment processes under the conditions specified in Table 2 are given in Figure 3.

In Figure 3a, it is seen that precipitate phase is not formed in the microstructure of the annealed (O) sample as a necessity of the process but some alloy elements do not dissolve (segregation) and thus, the structure has porosities. However, in the samples treated with T6, RRA and HTPP heat treatment processes (Figure 3b, c, d), secondary phase precipitates are observed with the effect of aging. Besides, considering the grain structures of samples which underwent different heat treatments, the most coarse-grained microstructure is obtained through the annealing (O) process. It is also understood from SEM images given in Figure 3 that grain sizes of samples treated with HTPP and RRA heat treatments are bigger than those of samples treated with T6 heat treatmen process. This is because of the fact that grain sizes of samples increase as they re-interact with heat during the pre-precipitate formation process performed for 30 minutes at 450°C after the T6 heat treatment in HTPP and RRA heat treatment processes as well as one-hour solution treatment at 220°C and 24-hour secondary aging process at 120°C in RRA heat treatment [19]. SEM images of Figure 3 also reveal that secondary phase precipitates are formed in the structure at nano dimension through different aging processes. As reported in a previous research, secondary phase precipitates can form both in the grain centers and along the grain boundries in the microstructure via aging heat treatments [22].

3.2 Hardness measurements

Hardness values of 7075 aluminum alloys which were annealed and aged through different heat treatment processes (T6, RRA and HTPP) are given in Figure 4. While average hardness was measured as 68 HB in the annealed samples, it was determined that hardness values of aged samples were almost two times higher than the hardness values of annealed samples. Hardness measurements revealed that the hardness of alloy changes depending on the type of aging. While the highest hardness values were obtained in the samples treated with T6 heat treatment process (168 HB), samples which underwent RRA and HTPP heat treatment processes displayed similar values with 156 HB and 157 HB, respectively. This decrease in the hardness is attributed to the dimensional increase (growth

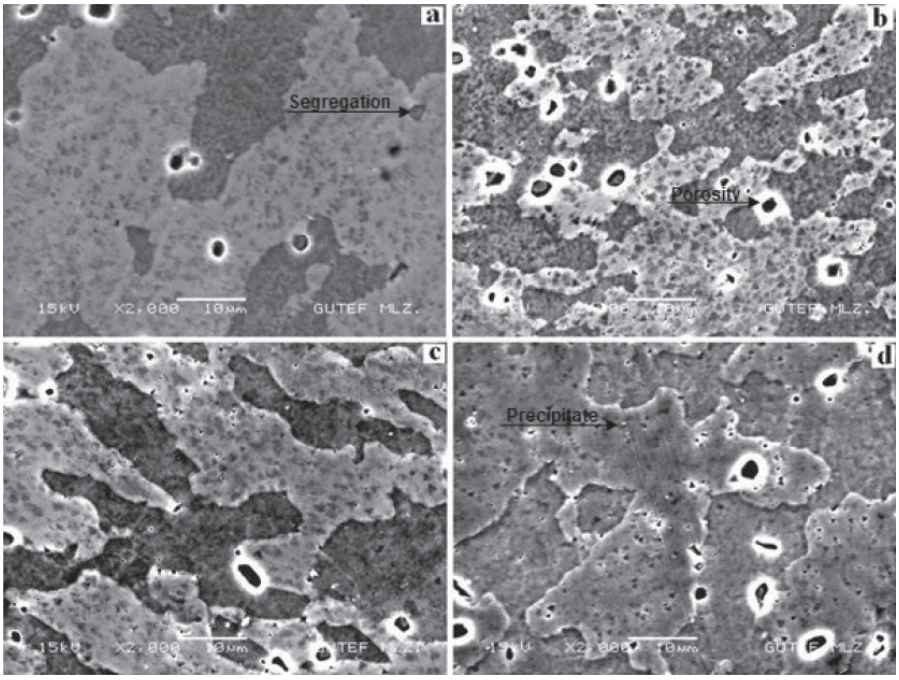

Fig. 3: SEM images of the AA7075 alloy treated with different heat treatment processes O (a), T6 (b), HTPP (c) and RRA (d).

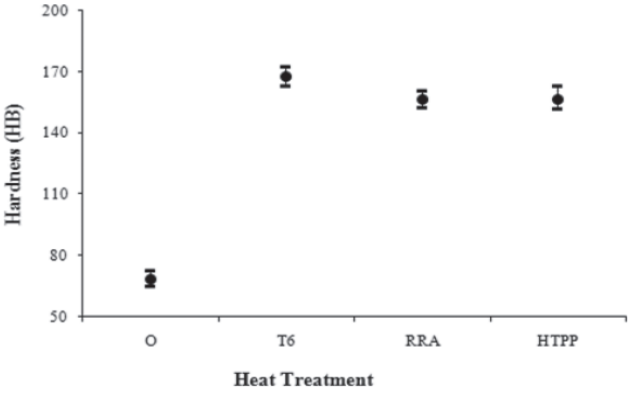

Fig. 4: Hardness changes of the AA7075 alloy aged through different heat treatment processes

of precipitates) of η (Mg_2Zn) precipitates which are already available in the structure through re-heating of the samples during solution treatment and re-aging stages in RRA heat treatment following T6 process as well as high temperature pre-precipitate formation stage in HTPP heat treatment. In T6 heat treatment, the alloy which is solution treated for 2 hours at 485°C and water quenched at room temperature displays a saturated solid solution structure. The secondary phase precipitates formed in the matrix through artificial aging increase the strength of matrix [18]. Secondary phase particulates forming in the structure increase the hardness of the material. These hardness values obtained in the present study are also in parallel to the findings of some previous studies [23, 24].

3.3 XRD examinations

Results of XRD analysis obtained at 2θ, $30° \leq 2\theta \leq 90°$ interval for the diffraction angle of samples treated with different heat treatments (O, T6, RRA, HTPP) are given in Figure 5. It is expected that secondary phase precipitates which enhance strength are formed in the structure of alloy with these different aging heat treatment processes. Aging processes of 7075 aluminum alloy lead to some phase transformations in the structure. At the end of XRD analyses, as expected, semi coherent ή ($MgZn_2$) phase which enhances strength, incoherent and stable η (Mg_2Zn) phase and $MgAl_2O_4$ phase which is thought to be formed at production stages are observed in the structures of the aged samples. It is stated by Vargas in a study [25] that $MgAl_2O_4$ type inclusions can also be observed in the structure. However, it was determined that $Mg_{0.971}Zn_{0.025}$ ve $(Mg_{0.76}Zn_{0.25})O$ phases which were not addressed much in the literature were also present in the structure as a result of aging heat treatment processes. Furthermore, such elements as Al and Fe are also observed in the structure. Presence of Al and Fe in the structure demonstrates the segregations occuring at the production stages of AA7075 alloy (Figure 3).

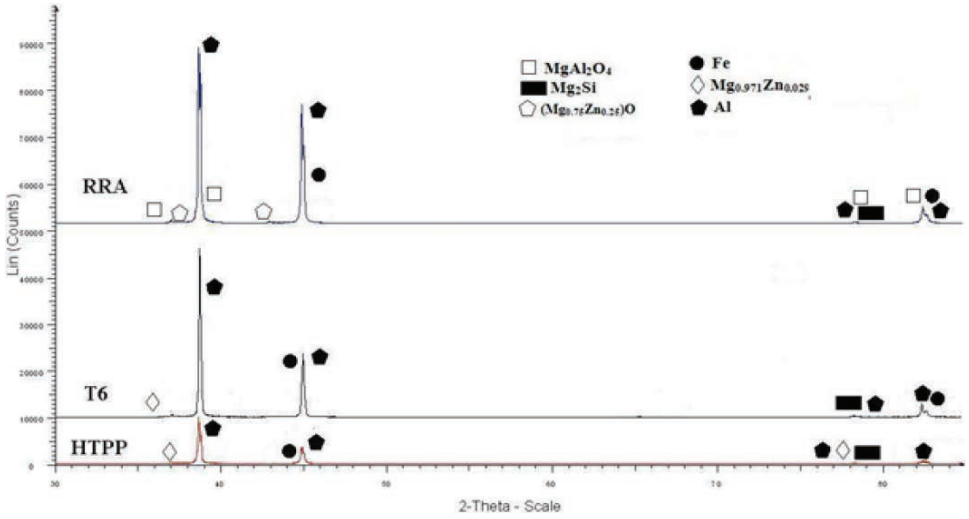

Fig. 5: XRD results of the aged (HTPP, T6, RRA) AA7075 alloy

Some previous studies have also reported the formation of different phases together with η ($MgZn_2$) phase in the structure during the aging processes [24, 18, 19]. These phases can precipitate both within the grains and along the grain boundries. These phases formed during the production stages of the alloy do not dissolve completely in the structure with the solution treatment process prior to the aging processes [26]. Saturated solid solution contains undissolved alloy elements in it even in small amounts. Thus, it is really difficult to claim that all phases detected as a result of XRD examinations were formed during the aging processes. On the other hand, no matter what are the conditions, the presence of these intermetallics in the structure following aging is inevitable.

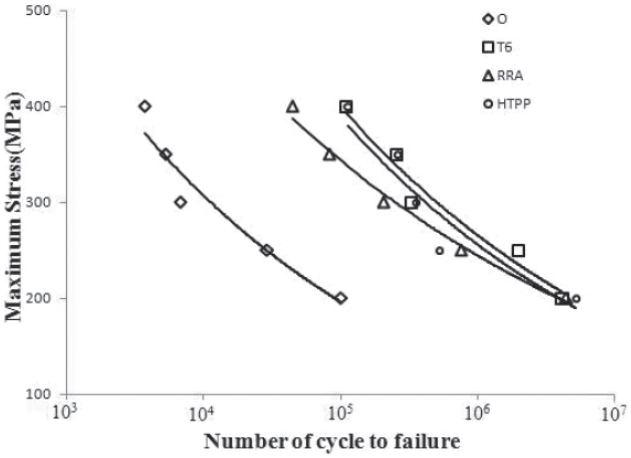

Fig. 6: S – N diagram obtained at the end of fatigue tests of the AA7075 aluminum alloy aged through O, T6, RRA and HTPP heat treatment processes

3.4 Fatigue tests

The mean of the values obtained at the end of fatigue tests was calculated and the strain (S) – number of cycles (N) diagram was drawn. S – N diagram obtained at the end of fatigue tests of the AA7075 aluminum alloy aged through O, T6, RRA and HTPP heat treatment processes was presented in Figure 6.

In accordance with the S – N diagram given in Figure 6, it is clear that the fatigue curve of the annealed (O) samples differs from those of the samples aged through the application of other heat treatment processes (T6, RRA, HTPP). This means that fatigue strength of the annealed samples is relatively lower than the samples aged at different conditions. The highest fatigue cycle was observed in the samples which underwent T6 heat treatment. It was determined that the numbers of cycle and fatigue strengths of the samples treated with HTPP and RRA processes were considerably close to one another. Although fatigue strengths and numbers of cycle of the samples aged through RRA and HTPP processes are higher than the annealed (O) samples, they are lower than those of the samples aged through T6 heat treatment. These changes in the fatigue strengths are attributed to the dimensional increase (growth of precipitates) of η (Mg_2Zn) precipitates which are already available in the structure through re-heating of the samples during solution treatment and re-aging stages in RRA heat treatment following T6 process as well as high temperature pre-precipitate formation stage in HTPP heat treatment. Considering the fatigue strength in the cycle for 10^5 number of cycle, it is

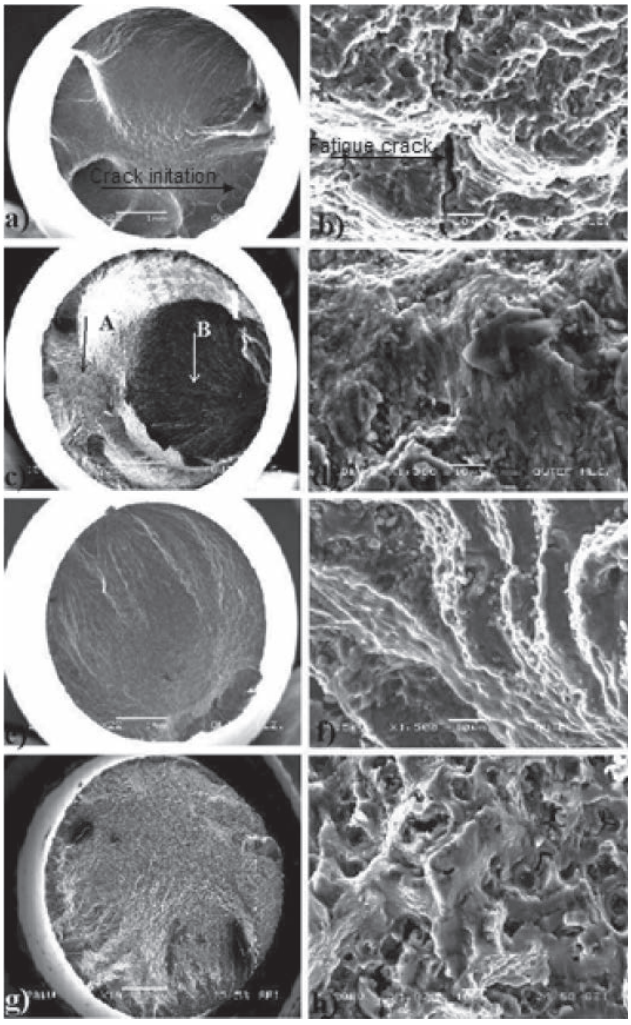

Fig. 7: SEM images of broken surfaces formed at the end of fatigue tests O (a, b), T6 (c, d), RRA (e, f), HTPP (g, h).

seen that the fatigue strength of the samples aged at different conditions has increased by about 40% when compared to the fatigue strength of the annealed samples. Considering 10^6 number of cycle (when fatigue strength values of annealed samples are considered), it was determined that the fatigue strength has increased by about 38% in the samples treated with RRA process. On the other hand, the samples treated with HTPP heat treatment process displayed fatigue strength values close to the samples in T6 heat treatment.

Fructured surface SEM images of the experimental samples following the fatigue tests are given in Figure 7. It is also seen in Figure 7c, d that the fracturing was semi-ductile in the sample aged through T6 heat treatment. Cracks which start in the external surfaces (A direction) grow in parallel to the increase in the number of cycle and lead to the fracturing of the material (in the area indicated with B, fracturing area). It is understood that fracturing of the samples aged through RRA (Figure 7e, f) and HTPP (Figure 7g, h) heat treatment has a more ductile fracturing mode in comparison to the samples aged with T6 heat treatment. Big cavities formed on the sample surface represent a ductile fracturing. Micro cracks which start on the sample surface with the effect of load and number of cycle during the fatigue tests grow towards the center, unite and form macro cracks and these macro cracks cause fracturing after a certain cycle.

Fatigue cracks, inclusions and second phase particulates formed in the structure through aging are observed on the broken surfaces. Inclusions generally occur 10 μm below the surface. In a study conducted by Shadzad et al. on the same alloy, they emphasize that micro cracks emerging during the fatigue start from these inclusions or areas close to them [27]. When fractured surfaces given in Figure 6 are examined, it is obviously seen that micro cracks start from areas where inclusions, coarse secondary phase particulates and microstructural defects are present. Besides, some alloy elements remaining undissolved in the structure during the solution treatment are also found in the structure. Micro cracks developing during the fatigue tests preferentially develop between the alloy elements found undissolved in the structure and the matrix.

4 Conclusion

The conclusions obtained at the end of the experimental studies can be drawn from this study:

1. It was determined that hardness changed in the samples treated with different heat treatment process (O, T6, RRA, HTPP) depending on the selected process. The highest hardness value was measured in the samples to which T6 heat treatment was applied while hardness values measured in the samples treated with HTPP and RRA processes followed it.
2. As it was expected, XRD examinations revealed that secondary phase (Mg_2Zn) precipitates were formed through aging. Besides, $Mg_{0.971}Zn_{0.025}$ ve $(Mg_{0.76}Zn_{0.25})O$ phases which had not been addressed much in the literature until that time were also detected.
3. It was seen that fatigue strength changed depending on the heat treatment applied to the sample at the end of the fatigue tests. While the highest fatigue strength was recorded in samples treated with artificial aging (T6) process, the lowest fatigue strength was measured in the annealed samples.

4. It was determined in fatigue fractured surface SEM examinations that micro cracks which cause fracturing start from areas where inclusions, coarse secondary phase particulates and microstructural defects are present or in the areas very close to these regions and lead to fatigue fracture.

Received: September 22, 2012. Accepted: November 16, 2012.

References

[1] Z.X. Wang, Y.A. Zhang, B.H. Zhu, H.W. Liu, F. Wang, B.G. Xiong, *Trans. Nonferrous Met. Soc. China* **16** (2006), 808–812.
[2] H. Aydın, A. Bayram, M.T. Yıldırım, K. Yigit, *Mater. Sci-Medzg.* **16-4** (2010), 311–319.
[3] R.H. Oskouei, R.N. Ibrahim, *Mater. Sci. Eng. A* **528** (2011), 1527–1533.
[4] P. Cavaliere, F. Panella, *J. Mater. Proces. Technol.* **206** (2008), 249–255.
[5] J.F. Li, Z.W. Peng, C.X. Li, Z.G. Jia, W.J. Chen, Z.Q. Zheng, *Trans. Nonferrous Met. Soc. China* **18** (2008), 755–762.
[6] P.S. De, R.S. Mishra, C.B. Smith, *Scripta Mater.* **60** (2009), 500–503.
[7] Y. Xue, H. El-Kadiri, M.F. Horstemeyer, J.B. Jordon, H. Weiland, *Acta Mater.* **55** (2007), 1975–1984.
[8] K.S. Al-Rubaie, E.K.L. Barroso, L.B. Godefroid, *Mater. Sci. Eng. A* **486** (2008), 585–595.
[9] H. Ji, L. Yuan, D. Shan, *J. Mater. Sci. Technol.* **27-9** (2011), 797–901.
[10] S.L. Winkler, H.M. Flower, *Corros. Sci.* **46** (2004), 903–915.
[11] M. Baydogan, H. Cimenoglu, E.S. Kayalı, *Wear* **257** (2004), 852–861.
[12] L.P. Huang, K.H. Chen, S. Li, M. Song, *Scripta Mater.* **56-4** (2007), 305–308.
[13] A. Somoza, A. Dupasquier, *J. Mater. Sci. Technol.* **135** (2003), 83–90.
[14] G. Waterloo, V. Hansen, J. Gjonnes, S.R. Skjervold, *Mater. Sci. Eng. A* **303** (2001), 226–233.
[15] L.K. Berg, J. Gjonnes, V. Hansen, X.Z. Li, M. Knutson-Wedel, G. Waterloo, D. Schryvers, L.R. Wallenberg, *Acta Mater.* **49** (2001), 3443–3451.
[16] D. Godart, E. Archambault, E. Aeby-Gautier, G. Lapasset, *Acta Mater.* **50-9** (2002), 2319–2329.
[17] A. Fakıoglu, An investigation of fatigue behaviour of aged AA7075 aluminium alloys, *M.Sc. Thesis* (January 2012).
[18] D. Özyürek, R. Yılmaz, E. Kibar, *J. Fac. Eng. Archit Gaz.* **27-1** (2012), 193–203.
[19] R. Yılmaz, D. Özyürek, E. Kibar, *J. Fac. Eng. Archit Gaz.* **27-2** (2012), 429–438.
[20] S. Theng-Shih, C. Ouin-Yang, *Mater. Sci. Eng. A* **348** (2003), 333–344.
[21] S. Theng-Shih, W.S. Liu, Y.J. Chen, *Mater. Sci. Eng. A* **325** (2002), 152–162.
[22] A. Abolhasani, A. Zarei-Hanzaki, H.R. Abedi, M.R. Rokni, *Mater. Design* **34** (2012), 631–636.
[23] A.S. El-Amoush, *J. Alloy. Compd.* **465** (2008), 497–501.
[24] S.W. Kim, D.Y. Kim, W.G. Kim, K.D. Woo, *Mater. Sci. Eng. A* **304–306** (2001), 721–726.
[25] M. Vargas, S. Lothabai, *Rev. Rom. Mater.* **12-2** (2010), 270–277.
[26] N. Mahathaninwong, T. Plookphol, J. Wannasin, S. Wisutmethangoon, *Mater. Sci. Eng. A* **532**, (2012), 91–99.
[27] M. Shahzad, M. Chaussumier, R. Chieragatti, C. Mabru, F.R. Aria, *J. Mater. Sci. Technol.* **210** (2010), 1821–1826.